Chalcogenide Letters Vol. 21, No. 2, February 2024, p. 151 - 159

Optical and electrical properties of Ni^{+2} doped nanocrystalline Bi_2S_3 thin films prepared by chemical bath deposition method

M. A. Hussain[a,*], P. J. Saikia[b], S. R. Devi[a], L. R. Singh[c]
[a]*Department of Physics, Presidency College, Motbung-795107, Manipur, India*
[b]*Department of Electronics, Jagannath Barooah College (Autonomous), Jorhat-785001, Assam, India*
[c]*Department of Physics, D.M. College of Science, Imphal-795001, Manipur, India*

Nickel (Ni^{+2}) doped nanocrystalline Bi_2S_3 thin films are deposited on the glass substrate from the solutions containing Bismuth Nitrate, Ethylenediamine Tetraacetic acid (EDTA) and Thioacetamide at a bath deposition temperature of 318K. The optical, surface morphological and electrical properties of Ni-doped Bi_2S_3 thin films prepared at three different doping concentration are investigate by using ultraviolet–visible transmission spectra (UV–Vis), Scanning electron microscopy (SEM), Energy Dispersive X-ray (EDAX) and thermo-e.m.f. techniques. The optical band gap energies are found in between 2.32-2.43 eV. The SEM images show that the prepared films are continuous, dense and distributed over the entire area with good uniformity. The electrical conductivity of the films are in the order of $10^{-2}\Omega^{-1}m^{-1}$. The films are n-type as determined from the Hot Probe method. Photoconductivity studies reveal that photocurrent increases with the increase in Ni doping concentrations. Due to the absorption of photons, free electron-hole pairs (EHP) are produce.

(Received October 27, 2023; Accepted February 5, 2024)

Keywords: Nanocrystalline, Thin films, Optical, Electrical and thermometer

1. Introduction

In the last two decades, nanocrystalline thin films have developed in scientific research due to their future potential application in the various fields of electronic devices. The properties of the materials are entirely dependent upon the particle or grain size. The optical, electrical and magnetic properties can be changed by changing the particle or grains size. These unusual properties are required for the development of modern electronic devices such as solar cell, integrated circuit, etc. Among the many semiconductor compounds, group V-VI semiconductor compounds are consider an important material for potential application in photosensitivity, photoconductivity and thermoelectric power [1–3].These compounds also widely used in optoelectronic devices, electrical switching, solar selective, decorative coatings etc. [4]. Out of these V–VI compounds semiconductor, bismuth sulphide (Bi_2S_3) is a promising candidate for optoelectronic devices as its band gap of 1.7 eV in bulk material that lies in the visible solar energy spectrum and could be increase to higher energy by reducing the particle or grain size [5-7]. Several researchers have reported for the preparation of nanocrystalline Bi_2S_3 thin films using different techniques such as vacuum evaporation [8-11], cathodic electro-deposition [12], anodic electrodeposition [13], hot-wall method [14], solution gas interface [15], spray deposition [16-17] etc. Among the above various techniques of thin film preparation, we preferred chemical bath deposition, which is simple, economic, suited for a large area deposition and does not required for sophisticated instrument. Chemical deposition of Bi_2S_3 thin films have reported earlier by many authors using different sulphide ion releasing sources such as thiosulfate, thiourea and thioacetamide [18–23]. Characterization of the as-prepared and annealed films of the undoped nanostructured Bi_2S_3 thin films prepared by chemical bath deposition technique using thioacetamide (TAM) as sulphide ion source and triethanolamine (TEA) as complexing agent have

* Corresponding author: hussainmakak@gmail.com
https://doi.org/10.15251/CL.2024.212.151

reported in our earlier paper [24]. The literature available for doped Bi_2S_3 thin films with element such as nickel [25], manganese [26], antimony [27-29], lead [30], copper [31-32], iron [33] graphene [34-35] etc. However, there is a limited literature available on the optical and electrical properties of Ni doped nanocrystalline Bi_2S_3 thin films. In this paper, we represent a comprehensive study in optical, morphology, electrical and photoconductivity properties of Ni-doped Bi_2S_3 thin films.

2. Preparation of Ni-doped nanocrystalline Bi_2S_3 thin films

For the preparation of Ni-doped nanocrystalline Bi_2S_3 thin films, Bismuth nitrate ($Bi(NO_3)_3$), Thioacetamide ($CH_2CS.NH_2$), and $Ni(NO_3)_2$ are used as Bi^{+3}, $S^{-2}$and Ni^{+2} ions sources respectively. Triethanolamine (TEA) ($C_6H_{15}NO_3$) is used as a complexing agent. For this, 5ml of 0.5M $Bi(NO_3)_3$ and 1.5wt% of $Ni(NO_3)_2$ is mixed with 2ml of TEA and stirred for 20 min at 300K to dissolve $Bi(NO_3)_3$ and $Ni(NO_3)_2$ into the solution. Consequently, 4ml of $CH_2CS.NH_2$ is added to the resultant solution and further stirred for 2 min to get a uniform mixture solution. Lastly, 39 ml of double distilled water is added to the resultant solution to obtain a total volume of 50 ml. Then, tin chloride-treated glass substrates are dipped vertically in the resultant solution supported by the wall of the beaker and heated at 318K for 20 min with the help of the hot plate of a magnetic stirrer. A thermometer is placed in the solution to measure the temperature. On heating the colour of the solution changes from dark orange to dark brown, this indicates the initiation of reaction and formation of Bi_2S_3 nano particles. After heating for 20 min, the solution is kept at room temperature (300K) for 2 hr for further deposition. The glass substrates coated with Ni-doped Bi_2S_3 films are remove from the bath solution, cleaned with deionized water, and dried in an open atmosphere. The film on the substrate surface facing towards the wall of the beaker is retained for further studies and the other side is removed with dilute nitric acid. In the same procedure as discussed above, three sets of films of different doping concentrations viz 1.5wt%, 2wt%, and 2.5wt% of $Ni(NO_3)_2$ are prepared, and investigated their optical, electrical, and morphological properties.

For the studies of photoconductive rise and decay characteristics of the Ni-doped Bi_2S_3 thin film, Al electrodes are vacuum deposited on the two ends of rectangular Ni-doped Bi_2S_3 films separated by a small gap and a gap-type sample is mounted on the sample holder placed in the vacuum chamber. The experimental arrangement is shown in Fig.1. A constant voltage is applied to the sample through a standard resistance and is connected to the X-Y/t recorder (M/S Digital Electronics Ltd., Mumbai, India Model: Omnigraphic 2000). The voltage applied to the sample is recorded along the X-axis of the recorder and the potential drop across the standard resistance due to the current flowing through the sample is recorded along the Y-axis of the recorder. The chamber is evacuated before the experiment. First, the recorder is switched on and kept in a Y-t mode, and then high-intensity white light from the QTH lamp is allowed to fall on the sample for a short period of time.

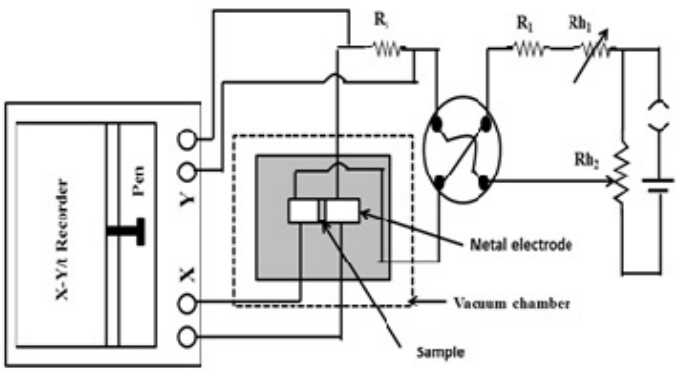

Fig. 1. Arrangement of X-Y/t recorder for measurement of photoconductive rise and decay.

The change in the Y-axis due to light 'on' and 'off' is recorded. A Luxmeter (Sigma 1010A) measures the intensity of light. The nature of the prepared Ni-doped Bi2S3 thin films is determined from the Hot Probe method and detailed procedure for measurement is discussed in our earlier paper [36]

3.1. Reaction mechanism for the growth of Ni-doped Bi_2S_3 thin films

The deposition process of Ni-doped nanocrystalline Bi_2S_3 thin film is based on the slow release of Bi^{+3} and S^{-2} ions in the solution which then condense ion by ion or cluster by cluster on the surface of the glass substrate. The rate of formation of Bi_2S_3 thin film is depend on the concentrations of Bi^{+3} and S^{-2} ions present in the precursor solution. The release of Bi^{+3} ions in the bath solution is controlled by TEA, which forms a complex $Bi[(TEA)]^{3+}$ with Bi^{+3}. In this solution different amount of nickel nitrate $Ni(NO_3)_2$ (viz 1.5wt%, 2wt% and 2.5wt%) is added. The reaction mechanism are given as follow

$$Bi(NO_3)_3.5H_2O + TEA \rightarrow [Bi(TEA)]^{+3} + 5H_2O + NO_3^- \quad (1)$$

$$[Bi(TEA)]^{+3} \rightarrow Bi^{+3} + TEA \quad (2)$$

$$CH_3CSNH_2 + OH^- \rightarrow CH_3CONH_2 + SH^- \quad (3)$$

$$SH^- + OH^- \rightarrow S^{-2} + H_2O \quad (4)$$

$$Ni(NO_3)_2 \rightarrow Ni^{+2} + NO_3^- \quad (5)$$

$$Bi^{3+} + Ni^{2+} + S^{2-} \rightarrow Bi_{2-x}Ni_xS_3 \quad (6)$$

3.2.Optical properties of Ni-doped Bi_2S_3 thin films

Fig.2 (a) shows the absorption spectra of Ni-doped nanocrystalline Bi_2S_3 thin films. It is evident from the figure that the absorbance increases with increasing in Ni doping concentration. Fig.2 (b) shows the $(\alpha h\nu)^2$ vs $(h\nu)$ plots for Ni-doped Bi_2S_3 thin films corresponding to different doping concentrations. Extrapolation of the linear portions of the plots to the energy axis yields the direct band gap values 2.32 eV to 2.43 eV for the Ni-doped nanocrystalline Bi_2S_3 thin films as given in Table 2.

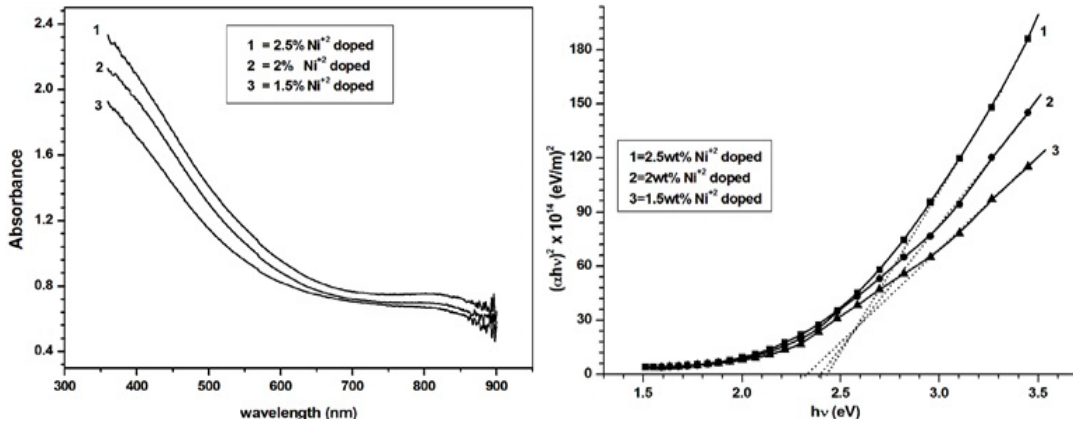

Fig. 2. (a) Plot of Absorbance vs wavelength of Ni-doped unannealed Bi_2S_3 thinfilms of different dopinng concentrations; (b) (a) Plot of $(\alpha h\nu)^2$ vs hv of Ni-doped unannealed Bi_2S_3 thinfilms of different doping concentrations.

It is observed that band gap increases with increase in Ni doping concentration. Incorporation of Ni to Bi_2S_3 creates some structural changes and the optical band gap is strongly dependent on fractional concentration of Ni atoms. This may be due to the tendency of Ni atoms to introduce high degree of disorder and hence higher densities of localized states in the forbidden gap [37].

3.3. Photoconductive rise and decay measurements of Ni doped Bi_2S_3 thin film

Fig.3 shows the rise and decay curves of Ni-doped Bi_2S_3 thin films at light intensity of 1700 Lux. It is observed that the photocurrent increases with the increase in Ni doping concentrations. Due to the absorption of photons free electron-hole pairs (EHP) are generated. The photo-generated electrons and holes in excess to the thermal equilibrium carriers are responsible for photoconduction process. The increase in photoconductivity has two main contributors viz, one from the resultant increase in the photo-generated carriers and the other from the increase in the effective mobility. With increase in Ni-doping concentration of the Bi_2S_3 films, grains boundary reduces resulting to more photoconductivity.

From Fig.3, it is observed that for all the Ni doped Bi_2S_3 films at three different concentrations the photocurrent rises very quickly on switching on the light source and then reaches a steady state. Fast rise time response may be attributed to the dominant fast process of photo generation of electron-hole pairs. The current reaches a steady value when the rate of recombination becomes equal to the rate of generation of new carriers and concentration of carriers reaches a steady value. When the light is switched off, electron-hole pair recombination process dominates, so the photocurrent decays slowly. The photoconductive rise time (τ_r) and decay time (τ_d) are determined from the tangents drawn to the photoconductive rise and decay curves. The values are founds to decrease with increase in doping concentrations and the estimated values of τ_r and τ_d are given in Table 1. The value of decay constant is determined from the slopes of $\ln I_t$ versus $\ln t$ curves shown in Fig.4 using the relation

$$I_t=I_o(1+at)^{-b}= I_o t^{-b} \quad (1)$$

where Io is the initial photocurrent at $t=t_{off}$ and It is the photocurrent after time 't' from t_{off} and b is the decay constant and the calculated values are given in the Table 1.

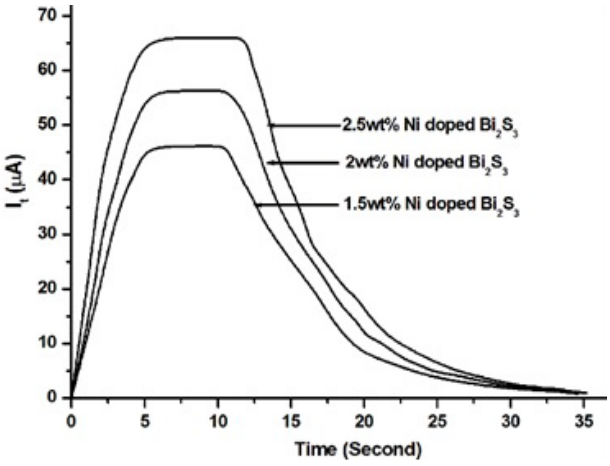

Fig. 3. Rise and decay of photocurrent with time for Ni-doped Bi_2S_3 thin films under illumination of 1700 Lux.

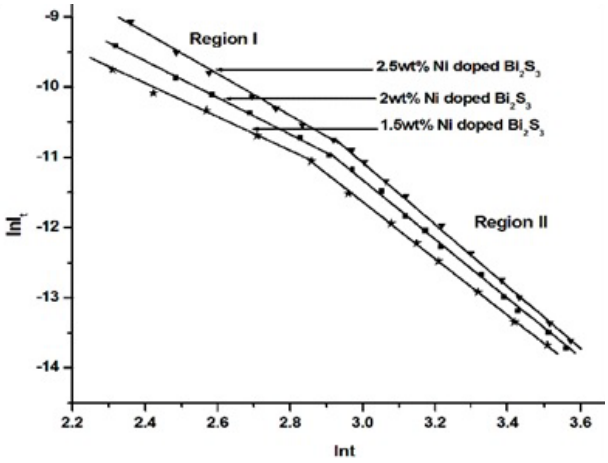

Fig. 4. Plot of lnI_t with lnt for Ni-doped Bi_2S_3 thin films.

3.4. Surface Morphology Studies

Scanning electron microscopy (SEM) photographs are used for studying the surface morphology of the films.Fig. 5(a-c) represents the Ni-doped Bi_2S_3 thin film at different concentrations viz 1.5wt%, 2wt% and 2.5wt%. It is observed that the films are continuous over the glass surface and are fairly uniform. The grains of the films have different shapes and sizes but almost compact. There are no macroscopic defects such as voids, peeling or cracks. From Fig.5, it is observed that small clusters are distributed throughout the surface. Agglomeration of small crystallites in the films are also evident from the photographs.

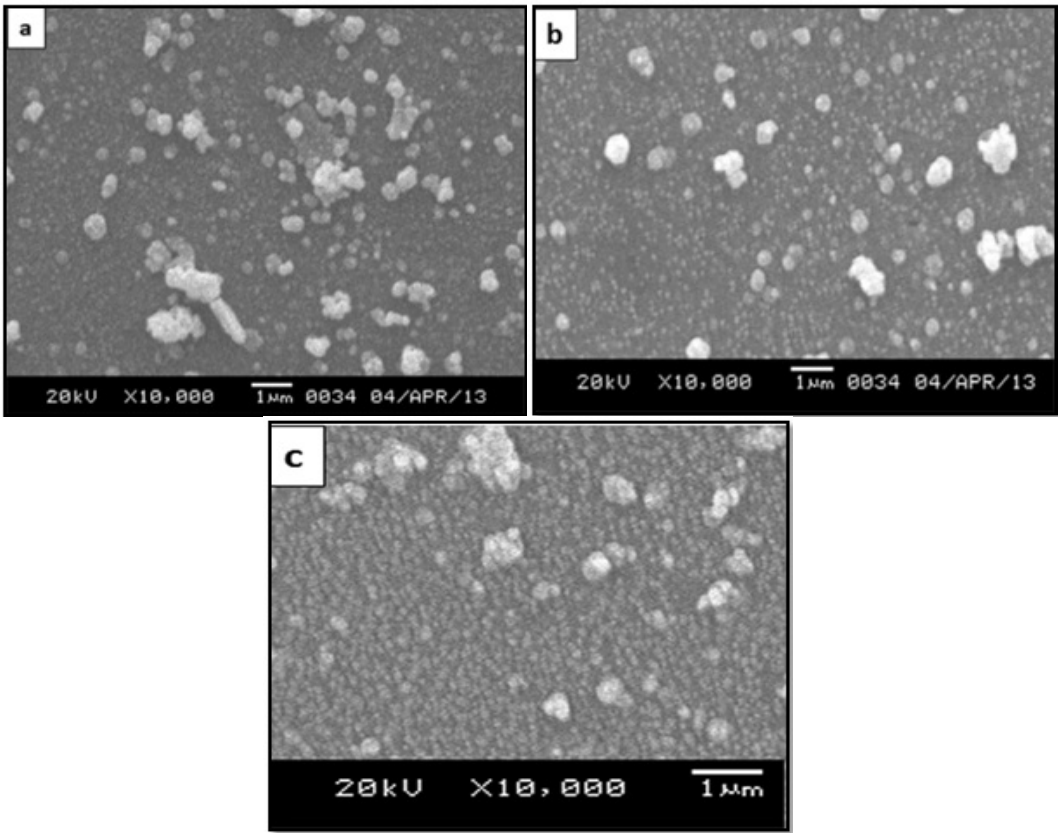

Fig. 5. SEM photographs of Ni-doped Bi_2S_3 thin film at different concentrations (a) 1.5wt%, (b) 2wt% and (c) 2.5wt%.

Such agglomeration makes it difficult to evaluate the grain size from SEM images andlarger grains are observed due to the coalesce of smaller clusters.All the films are continuous, compact, homogenous and free from voids, cracks or holes. From the photographs, it is observed that the grains are nearly spherical in shape and small clusters are observed in case of the higher doping concentration. Thus, the grains sizes decrease with increasing doping concentrations.

3.5. Energy dispersive X-ray analysis (EDAX) of Ni-doped Bi_2S_3 thin films

The quantitative and qualitative compositional analysis of the Ni-doped Bi_2S_3 film is carried out by EDAX technique. Fig.6(a-c). shows a typical EDAX pattern and details of relative analysis for three different Ni doping concentrations of Bi_2S_3 thin film. The spectrum confirms that Bi, S and Ni atoms are present in the prepared film. The average atomic percentage of Bi and S is found in between 34.93-37.7 and 61.36-58.18 respectively showing that the film is S deficiency. The average atomic percentage of Ni present in the prepared films increases with increase in doping concentrations.The extra peaks observed in the EDAX spectra correspond to Mg, Si, Na, Ca, Tc etc. which are due to glass substrate and or the substrate holder used in the EDAX instrument [38-40]. C and O peaks are also observed in the EDAX spectra, these might be due to exposure of the film to the atmosphere [41]. There is no source of these elements in the chemicals used for the Bi_2S_3 film synthesis. The prominent peak observed at around 1.9 keV in the EDAX spectra belong to Si which is due to glass substrate. We consider only the atomic% of Bi, S and Ni present in the spectra of doped sample neglecting the percentage of the other elements present in the spectra.

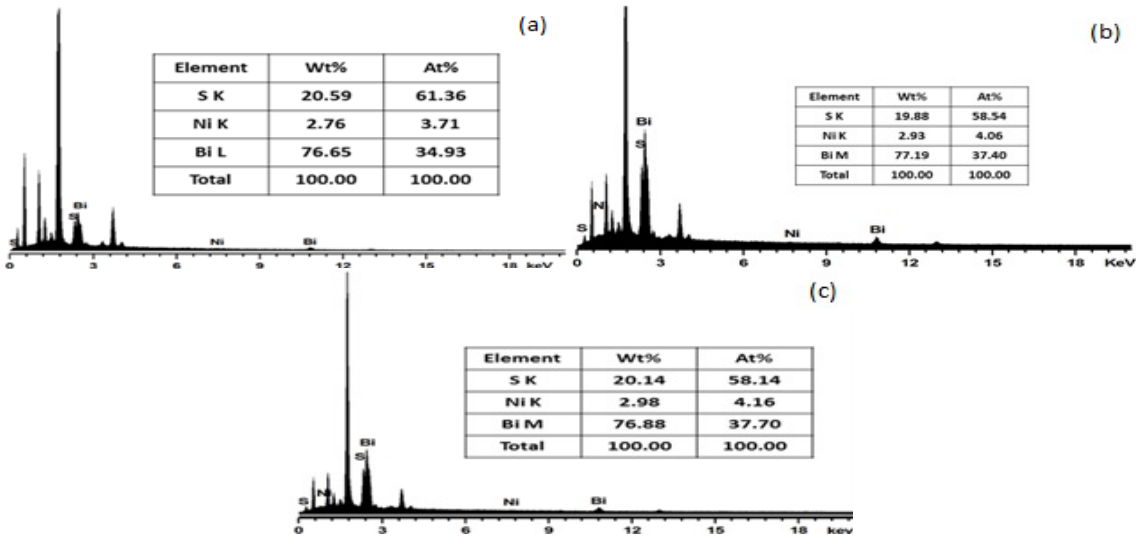

Fig. 6. EDAX spectra of (a) 1.5wt% (b) 2wt% (c) 2.5wt% Ni doped Bi_2S_3 thin film.

3.6. Temperature dependent electrical conductivity of Ni-doped Bi_2S_3 thin films

The variations of log(σ) with temperature for the Ni-doped nanocrystalline Bi_2S_3 are shown in Fig.7. The plots reveal two distinct regions: one below 378K, where the conductivity varies comparatively slowly with temperature and the other above 378K, where the conductivity varies rapidly with temperature. The thermal activation energy are calculated by using the relation

$$\sigma = \sigma_o e^{\frac{-E_a}{2kT}} \tag{2}$$

where E_a is the activation energy, σ_o is a constant, k_b is the Boltzman's constant and T is the absolute temperature. The conductivity increases with increase of Ni doping concentration because

of the increase of free–carriers. Ni dopingBi_2S_3thin films decreases in activation energy due to band tailing and reduces the height of the potential barrier between crystallites composing the films [42]. Electrical conductivity of a semiconductor is controlled by the number of charge carriers available for conduction. As the temperature increases from absolute zero, transitions are taking place between the defect levels and the conduction band and valence band [43]. The conductivity of the films are found to increase with increasing annealing temperature because the grain boundaries and the crystal lattice defects of the films are reduced with annealing temperature resulting in an increase of the mobility of the carriers. The electrical conductivity of the Bi_2S_3 films is found to be of the order of $10^{-3}\Omega^{-1}m^{-1}$.The calculated activation energy values are very small as compared with the observed band gap values. These energy levels are therefore thought to be associated with defect levels existing within the band gap.

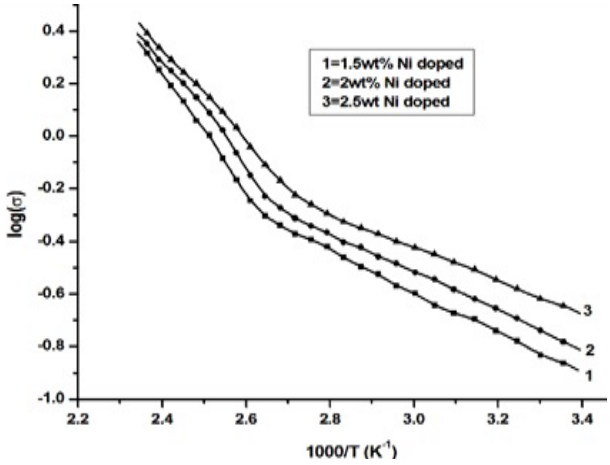

Fig. 7. Shows log σ versus 1000/T plots for Ni-doped Bi_2S_3thin films.

4. Conclusions

In the present investigation, Ni-doped nanocrystalline Bi_2S_3 thin films are successfully prepared by CBD technique and studied their optical, morphological, electrical and photoconductivity properties. The optical band gap for Ni-doped Bi_2S_3 films found to increase with increase in Ni-doping concentrations due to the increase in density of defects within the bandgap. The rise and decay curves of Ni-doped Bi_2S_3 thin films at light intensity of 1700 Lux shows that the photocurrent increases with the increase in Ni doping concentrations, due to the absorption of photons free electron-hole pairs (EHP) are generated. The quantitative and qualitative elemental analysis of the prepared thin films by XRF technique shows that the dopant element Ni is incorporate into the Bi_2S_3 films. Surface morphology studies by Scanning electron microscopy (SEM) reveal that the prepared Bi_2S_3 films have uniform surface morphology and well covered over the entire glass substrate without any void. It is also observed that the films consists of irregular shaped grains of random size and these irregular shaped nano grains are interconnected with each other to form a cluster. The electrical conductivity increases with increase in annealing temperature. The room temperature electrical conductivity found to be of the order of $10^{-3}\Omega^{-1}m^{-1}$.

Acknowledgements

We express our gratefulness to the Thin Film Research Laboratory, Department of Physics, Gauhati University, Guwahati for providing facilities of Uv-Visible spectrometer and Photo-conductivity measurement and SAIF, NEHU for SEM facilities.

References

[1] C. Ghosh, B.P. Varma, Solid State Communications 31(9), (1979), 683-686; https://doi.org/10.1016/0038-1098(79)90323-5

[2] F. Ding, Q.Wang, S. Zhou, G. Zhao, Y. Ye, R. Ghomashchi, R. Soc. Open Sci. 7 (2020) 200479; https://doi.org/10.1098/rsos.200479

[3] J.S. Curran, R. Phillippe, Proceedings of the 14th International Conference on ECVP Solar Energy, Stresa, 10-14 May (1982).

[4] J. Stuke, Journal of Non-Crystalline Solids 4 (1970) 1-26; https://doi.org/10.1016/0022-3093(70)90015-3

[5] A. Jana, C. Bhattacharya, S. Sinha, J. Datta, J. Solid State Electrochem. 13 (2008), 1339-1350; https://doi.org/10.1007/s10008-008-0679-z

[6] C.D. Lokhande, Materials Chemistry and Physics27(1) (1991) 1-43; https://doi.org/10.1016/0254-0584(91)90158-Q

[7] L.M. Peter, J. Electroanal. Chem., 98 (1979) 49; https://doi.org/10.1016/S0022-0728(79)80283-1

[8] J. Lukose and B. Pradeep, Solid State Commun., 78 (1991) 535-538; https://doi.org/10.1016/0038-1098(91)90371-2

[9] S. Mahmoud and F. Sharaf, FizikaA5 (1996) 205-213; https://doi.org/10.1002/(SICI)1097-0177(199603)205:3<213::AID-AJA1>3.0.CO;2-L

[10] K. Mageshwari, R. Sathyamoorthy, P. Sudhagar and Y.S. Kang,Appl. Surf. Sci., 257 (2011) 7245-7253; https://doi.org/10.1016/j.apsusc.2011.03.100

[11] K. Mageshwari and R. Sathyamoorthy, Vacuum, 86(2012) 2029-2034; https://doi.org/10.1016/j.vacuum.2012.04.006

[12] C. D. Lokhande and C.H. Bhosale, Bull. Electrochem., 6 (1990) 622.

[13] B. Miller, S. Menzes and A. Heller, J. Electroanal. Chem., 94 (1978) 85-89; https://doi.org/10.1016/S0022-0728(78)80326-X

[14] P. A. Krishnamoorthy and G. K. Shivkumar, Thin Solid Films, 121 (1984) 151; https://doi.org/10.1016/0040-6090(84)90237-2

[15] S. H. Pawar, P. N. Bhosale, M. D. Uplane and S. P. Tamhankar, Thin solid Films, 110 (1983) 165-170; https://doi.org/10.1016/0040-6090(83)90220-1

[16] S. H. Pawar, S. P. Tamhankar and C. D. Lokhande, Mater. Chem. Phys., 11 (1984) 401-412; https://doi.org/10.1016/0254-0584(84)90064-6

[17] S.A. Mahmoud, PhysicaB,301 (2001) 310-317; https://doi.org/10.1016/S0921-4526(01)00272-1

[18] A. U. Ubale, Mater. Chem. Phys., 121 (2010) 555-560; https://doi.org/10.1016/j.matchemphys.2010.02.021

[19] A. Jana, C. Bhattacharya, S. Sinha and J. Datta, J. Solid State Electrochem.,13 (2009) 1339-1350; https://doi.org/10.1007/s10008-008-0679-z

[20] R.R. Ahire and R. P. Sharma, Indian J. Eng. Mater. Sci., 13 (2006) 140-144.

[21] R.S. Mane, B. R. Shankapal and C. D. Lokhande, Mater. Res. Bull., 35 (2000) 587-601; https://doi.org/10.1016/S0025-5408(00)00244-0

[22] C.D. Lokhande, A. U. Ubale and P. S Patil, Thin Solid Films, 302 (1997) 1-4; https://doi.org/10.1016/S0040-6090(96)09540-5

[23] J.D. Desai and C. D. Lokhande, Mater. Chem. Phys., 41 (1995) 98-103; https://doi.org/10.1016/0254-0584(95)01538-8

[24] A. Hussain, A. Begum and A. Rahman, Materials Science in Semiconductor Processing 21 (2014) 74-81; https://doi.org/10.1016/j.mssp.2014.01.029

[25] R. Sakthivel, S. Kubendhiran, S.-M. Chen, Ultrasonic Sonochemical 54, (2019)68-78; https://doi.org/10.1016/j.ultsonch.2019.02.013

[26] N. Anasane, R. Ameta, Material Science 35, (2017)1; https://doi.org/10.1515/msp-2017-0032

[27] P. UshaRajalakshmi, Rachel Oommen, C. Sanjeeviraja, V. Ganesan, Superlattice Microstructure. 57, (2013) 158-165; https://doi.org/10.1016/j.spmi.2013.01.003

[28] S. Subramanian, Journal of Non-Crystalline Solids 356(23), (2010)1173-1179; https://doi.org/10.1016/j.jnoncrysol.2010.03.012

[29] P. Usha Rajalakshmi, R. Oommen, C. Sanjeeviraja, Thin Solid Films 531, (2013)76-80; https://doi.org/10.1016/j.tsf.2012.12.045

[30] V. Balasubramanian, N. Suriyanarayanan, Mater. Lett. 91, (2013)362-364; https://doi.org/10.1016/j.matlet.2012.09.099

[31] Arshad Hussain, R. Ahmed, Nisar Ali, Naser M AbdEl-Salam, Karim bin Deraman, Yong Qing Fu, Surf. Coat. Technol. 320, (2017)404-408; https://doi.org/10.1016/j.surfcoat.2016.12.012

[32]M.V. Yakushev, P. Maiello, T. Raadik, M.J. Shaw, P.R. Edwards, J. Krustok, A.V. Mudryi, I. Forbes, R.W. Martin, Thin Solid Films 562, (2014)195-199; https://doi.org/10.1016/j.tsf.2014.04.057

[33] R.S. Silva, H.D. Mikhail, E.V.Guimarães, E.R.Gonçalves, N.F. Cano, N.O.Dantas, Molecules 22(7), 2017)1142; https://doi.org/10.3390/molecules22071142

[34] Priyanka R. Jagadish, Mohammad Khalid, Lau Phei Li, Nowshad Amin, RashmiWalvekar, and Andy Chan., AIP Conf. Proc. 2137(1), 020004 (2019)

[35] O.K. Okoth, K Yan, Y Liu, J Zhang, Biosens. Bioelectron. 86, (2016)636-642; https://doi.org/10.1016/j.bios.2016.07.037

[36] A Hussain, A Begum and A Rahman, Indian J. Phys (August 2012) 86(8):697-701; https://doi.org/10.1007/s12648-012-0130-2

[37] N. F. Mott, and E. A. Davis, Electronics Processes in Non-Crystalline Materials, Clarendon, Oxford, 1979, p 428.

[38] Juan Chu, ZhengguoJin, Shu Cai, Jingxia Yang and Zhanglian Hong, Thin Solid Films, 520 (2012) 182-1831.

[39] R. Sahraei, S. Shahriyar, M. H. MajlesAra, A. Daneshfar and N. Shokri, Prog. Color Colorants Coat, 3 (2010) 82-90.

[40] S. Prabahar, and M. Dhanam, Journal Crystal Growth, 285 (2005) 41-48; https://doi.org/10.1016/j.jcrysgro.2005.08.008

[41] S. Mageswari, L. Dhivya, B. Palanivel and R. Murugan, Journal of Alloys and Compounds, 545 (2012) 41-45; https://doi.org/10.1016/j.jallcom.2012.08.010

[42] Sanjoy Paul, Istvan Gulyas, Ingrid L. Repins, Shin Mou, Jian V. Li,

[43] J. Lukose and B. Pradeep, Solid State Commun., 78 (1991) 535-538; https://doi.org/10.1016/0038-1098(91)90371-2